

# **ELEVATION-AZIMUTH SERVO SYSTEM SPECIFICATIONS FOR STAR TRACKING**

Charles F. White and James W. Titus

Equipment Research Branch  
Radar Division

April 12, 1956



**APPROVED FOR PUBLIC  
RELEASE - DISTRIBUTION  
UNLIMITED**

**NAVAL RESEARCH LABORATORY  
Washington, D.C.**

## CONTENTS

Abstract	ii
Problem Status	ii
Authorization	ii
INTRODUCTION	1
CELESTIAL AND TERRESTRIAL COORDINATES	1
AZIMUTH ANGULAR POSITION	3
AZIMUTH ANGULAR VELOCITY	4
AZIMUTH ANGULAR ACCELERATION	8
ELEVATION ANGULAR POSITION	9
ELEVATION ANGULAR VELOCITY AND ACCELERATION	11
FREQUENCY DOMAIN EQUIVALENT OF AZIMUTH TIME FUNCTION	15
AZIMUTH SERVO SYSTEM TRANSFER FUNCTION	15
AUTOMATIC TRACKING REQUIREMENTS STARTING FROM REST	18
PROPOSED SERVO SYSTEM	20
CONCLUSIONS	22
REFERENCES	23
APPENDIX A - TIME DOMAIN TO FREQUENCY DOMAIN TRANSFORMATION	24

## ABSTRACT

Radio astronomy star tracking requirements are resolved into elevation and azimuth coordinates and related to servo system transfer function specifications. Time functions for angular position, velocity, and acceleration are derived and maximum values found. A numerical example based upon the latitude of Washington, D. C., and a star declination such that at transit the angular distance from the zenith is 10 degrees or greater, is used in the calculation of the azimuth servo bandwidth needed to insure dynamic errors appropriate for automatic tracking with a 60-foot parabolic reflector (tracking error less than  $1/4$  degree). A bandwidth of a 0.1 radian per second is shown to be adequate. A block diagram is given for a servo system suitable for the azimuth coordinate.

## PROBLEM STATUS

This report completes one phase of the problem; work on other phases continues.

## AUTHORIZATION

NRL Problem R05-19

Manuscript submitted April 3, 1956

## ELEVATION-AZIMUTH SERVO SYSTEM SPECIFICATIONS FOR STAR TRACKING

### INTRODUCTION

The advent of radio astronomy has seen employed a wide variety of antennas and means for beam steering. Among these is the parabolic reflector mounted on a pedestal with elevation and azimuth coordinates of motion. Servo system requirements for such "EL-AZ" mounts become automatically defined upon specification of the tracking problem. In the study reported here, the tracking problem, a time-domain phenomenon, is transformed into the equivalent frequency domain function so that the servo systems may be designed using the frequency response method. In choosing the open-loop transfer functions for the servo systems several factors are considered, namely: (1) close fitting of the excitation function to achieve the maximum exclusion of noise simultaneous with adequate bandwidth for transmission of frequency components in the input signal, (2) suitable gain and phase margins to insure closed-loop servo system stability, and (3) the proper gain to insure that the maximum dynamic tracking errors almost equal but do not exceed the specified limits.

The derivation of time functions for elevation and azimuth angular position, velocity, and acceleration for star tracking is presented in the initial part of the body of the report. Guillemin's (1) method of approximating the frequency domain transform of a time function is then applied to the above-horizon portion of the azimuth time function. A transfer characteristic is then chosen following Graham's (2) procedure, in which the steady-state error series (3) plays a central role. The block diagram for a possible mechanization is given. The trajectory equations for the elevation axis are provided so that a similar study for the elevation coordinate servo may be made following the same procedure.

### CELESTIAL AND TERRESTRIAL COORDINATES

Star tracking angular position, velocity, and acceleration quantities resolved into elevation and azimuth coordinates are desired as a function of time. The location of maximum values of velocity and acceleration in both axes is also needed. In the derivations and in Fig. 1 a modification of the notation used by Hosmer (4) is employed.



Let

$z$  = interior angle of astronomical triangle at zenith, degrees

$T$  = hour angle ( $=\omega t$ )

$\omega$  = apparent angular velocity of the stars about earth's axis,

in radians per second =  $\frac{2\pi}{24 \cdot 3600} = 7.272 \cdot 10^{-5}$ , in

degrees per minute =  $1/4$

$t$  = time, seconds or degrees of rotation

$\theta$  = azimuth, degrees ( $\theta = -z$ )

$h$  = altitude (elevation angle), degrees

$\delta$  = declination, degrees

$\phi$  = latitude, degrees

#### AZIMUTH ANGULAR POSITION

To find the azimuthal quantities, start with Eq. (31), page 36 of reference 4,

$$\sin z = \frac{\sin T \cos \delta}{\cos h} \quad (1)$$

Substitute from Eq. (11), page 32 of reference 4,

$$\cos h = \frac{\sin \delta \cos \phi - \cos \delta \sin \phi \cos T}{\cos z} \quad (2)$$

and obtain

$$\frac{\sin z}{\cos z} = \frac{\sin T \cos \delta}{\sin \delta \cos \phi - \cos \delta \sin \phi \cos T} \quad (3)$$

$$\tan z = \frac{\sin T}{\cos \phi \tan \delta - \sin \phi \cos T} \quad (4)$$

Numerical evaluation of Eq. (4) gives an angle  $z$  which is  $180^\circ$  from the correct angle. This occurred through the use of the sine formula with its inherent ambiguity. Making this correction and the changes of variable  $T = \omega t$  and  $z = -\theta$ , we have

$$\tan \theta = \frac{-\sin \omega t}{A - B \cos \omega t} \quad (5)$$

where

$$A = \cos \phi \tan \delta$$

$$B = \sin \phi$$

#### AZIMUTH ANGULAR VELOCITY

Azimuth angle  $\theta$  as given by Eq. (5) may be differentiated to obtain the corresponding angular velocity. Thus,

$$\sec^2 \theta \frac{d\theta}{dt} = \frac{(A - B \cos \omega t)(-\omega \cos \omega t) + B\omega \sin^2 \omega t}{(A - B \cos \omega t)^2} \quad (6)$$

$$= \frac{-A \omega \cos \omega t + B \omega}{(A - B \cos \omega t)^2} \quad (7)$$

$$\frac{d\theta}{dt} = \frac{\cos^2 \theta \tan^2 \theta}{\sin^2 \omega t} [B - A \cos \omega t] \omega$$

$$\dot{\theta} = \omega \frac{\sin^2 \theta}{\sin^2 \omega t} [\sin \phi - \cos \phi \tan \delta \cos \omega t] \quad (8)$$

Azimuthal angular velocity is given by Eq. (8) except at points where  $\sin \omega t = 0$ . For these points, return to Eq. (7) and write

$$\left. \frac{d\theta}{dt} \right|_{t=0} = \frac{\omega}{\sin \phi - \cos \phi \tan \delta} \quad (9)$$

Figure 2 shows the azimuth angular velocity as calculated for  $t = 0$  using Eq. (9) and a latitude  $\phi = 39^\circ$  (approximately the latitude of Washington, D. C.). The extreme values shown,  $\delta = \phi \pm 10^\circ = 39^\circ \pm 10^\circ = 49^\circ$  and  $29^\circ$ , are hereafter referred to as Case 1 and Case 2 respectively. Since Case 2 exhibits a higher absolute value of azimuth velocity for a given approach to the zenith, detailed calculations are made for Case 2. Returning to Eq. (5), the constants become

Case 2

$$\phi = 39^\circ$$

$$\delta = 29^\circ$$

$$A = \cos 39^\circ \tan 29^\circ = 0.77715 \cdot 0.55431 = 0.43078$$

$$B = \sin 39^\circ = 0.62932$$

Figure 3 shows Eq. (5) calculated for Case 2 over a 24-hour period. The indicated points corresponding to the star rising and setting are from calculations shown later in the report. Using Eq. (9), the maximum azimuthal angular velocity becomes

Case 2

$$\begin{aligned} \left. \frac{d\theta}{dt} \right|_{t=0} &= \frac{7.272 \cdot 10^{-5}}{0.62932 - 0.43078} \\ &= \frac{7.272 \cdot 10^{-5}}{0.19854} = 0.3663 \text{ radian per second} \end{aligned}$$

Thus, for Case 2, at  $t = 0$  the azimuth angle is  $\theta = 180^\circ$  and the angular velocity is  $\dot{\theta} = 0.3663$  radian per second = 1.259 degrees per minute. For  $\delta < \phi$  (as in Case 2), the azimuth angle increases continuously from star rise to set. For  $\delta > \phi$  (as in Case 1), the azimuth angular rate is initially positive but reverses twice before the star sets.

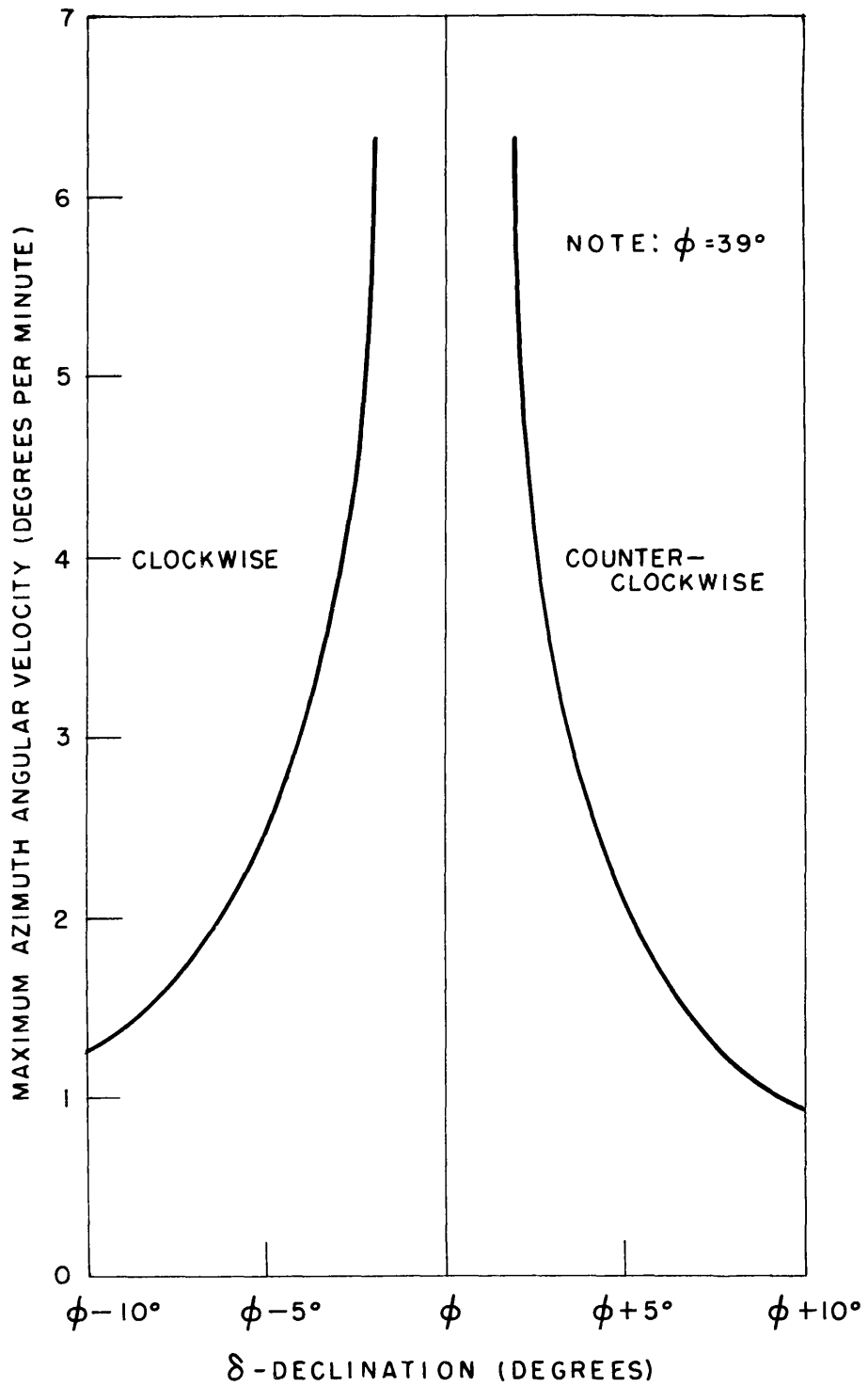


Fig. 2 - Maximum azimuth angular velocity as a function of star declination for a latitude of 39° North

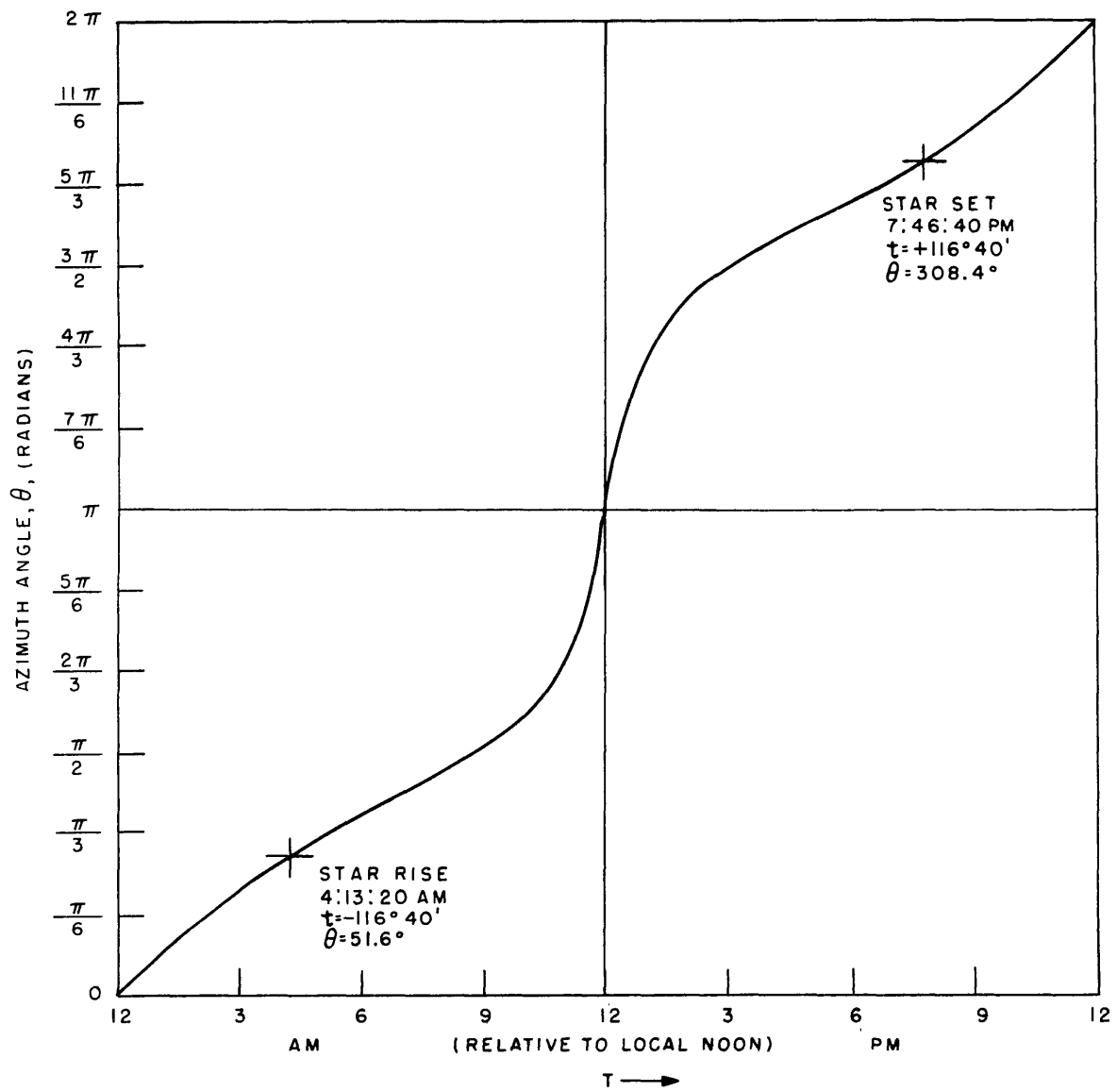


Fig. 3 - Azimuth angle versus time for  $\delta = 29^{\circ}$  and  $\phi = 39^{\circ}$

Of interest in servo system design is the relative period during which the input angular velocity is less than the minimum velocity of the servo motor, as installed in the mount. Good design may yield a dynamic range, or ratio of maximum to minimum motor speed, as high as 100 to 1; thus the region of inputs where the rate is less than 1% of the maximum may be called the "near-zero rate region." This region is related to star tracking in the azimuth coordinate from a station in the northern hemisphere as follows:

- a. Stars with south declination and stars with north declination less than the latitude of the tracking station exhibit continuous azimuth rates from east through south to west, with minimum values at star rise and star set.
- b. Stars with north declinations greater than the latitude will exhibit two regions of near-zero rate.
- c. A single continuous region of near-zero azimuth rate occurs for stars of declination approximately equal to 90° North.
- d. The relative duration of the regions of near-zero rate increases with declination from zero, for stars with declination equal to latitude, to 100% for stars with declinations approximately equal to 90° North.

#### AZIMUTH ANGULAR ACCELERATION

To find angular acceleration in the azimuth coordinate, differentiate Eq. (8) with respect to time and obtain, after simplification,

$$\frac{d^2\theta}{dt^2} = \frac{\omega \sin 2\theta}{\sin^2 \omega t} \left[ \sin \phi - \tan \delta \cos \phi \cos \omega t \right] \frac{d\theta}{dt} + \frac{\omega^2 \sin^2 \theta}{\sin^3 \omega t} \left[ \tan \delta \cos \phi (1 + \cos^2 \omega t) - 2 \sin \phi \cos \omega t \right] \quad (10)$$

Equation (10) set equal to zero may be solved for the time corresponding to the maximum value for angular velocity in azimuth. The values  $t = 0$ ,  $\theta = 0^\circ$  or  $180^\circ$  are found to be mathematically and intuitively correct. Accordingly, the azimuthal angular velocities previously calculated for  $t = 0$  are the maximum rates (as indicated on Fig. 2) for stars passing tangent to a  $10^\circ$  radius circle about the zenith.

Maximum azimuthal acceleration is found in the vicinity of  $\omega t = 7.5^\circ$  either side of star transit. By finding the slope between values of  $\dot{\theta}$  calculated for  $\omega t = 5^\circ$  and  $\omega t = 10^\circ$ , a value  $\ddot{\theta} = 4.28 \cdot 10^{-6}$  degrees per second per second was computed for the maximum acceleration. The velocity at this time is  $\dot{\theta} = 1.55 \cdot 10^{-2}$  degrees per second.

#### ELEVATION ANGULAR POSITION

Using Eq. (30) (reference 4, page 35), we write for the elevation angle

$$\sin h = \cos(\phi - \delta) - 2 \cos \phi \cos \delta \sin^2 \frac{\omega t}{2} \quad (11)$$

$$= C - D \sin^2 \frac{\omega t}{2} \quad (12)$$

#### Case 1

$$\phi = 39^\circ$$

$$\delta = 49^\circ$$

$$\begin{aligned} C &= \cos(\phi - \delta) = \cos(39^\circ - 49^\circ) \\ &= \cos(-10^\circ) = 0.98481 \end{aligned}$$

$$\begin{aligned} D &= 2 \cos \phi \cos \delta = 2 \cos 39^\circ \cos 49^\circ \\ &= 2 \cdot 0.77715 \cdot 0.65606 = 1.01971 \end{aligned}$$

#### Case 2

$$\phi = 39^\circ$$

$$\delta = 29^\circ$$

$$C = \cos 10^\circ = 0.98481$$

$$D = 2 \cdot 0.77715 \cdot 0.87462 = 1.35942$$

Star rise and star set occur at zero elevation. From Eq. (12), this occurs at

$$C = D \sin^2 \frac{\omega t}{2} \quad (13)$$

$$\sin^2 \frac{\omega t}{2} = \frac{\cos(\phi - \delta)}{2 \cos \phi \cos \delta} = \frac{\cos \phi \cos \delta + \sin \phi \sin \delta}{2 \cos \phi \cos \delta} \quad (14)$$

$$\omega t = 2 \sin^{-1} \left[ \frac{1 + \tan \phi \tan \delta}{2} \right]^{1/2} \quad (15)$$

Case 1

$$\begin{aligned} \omega t &= 2 \sin^{-1} \left[ \frac{1 + \tan 39^\circ \tan 49^\circ}{2} \right]^{1/2} \\ &= 2 \sin^{-1} \left[ \frac{1 + 0.80978 \cdot 1.1504}{2} = 0.96579 \right]^{1/2} \\ &= 2 \sin^{-1} 0.98273 = 2(\pm 79^\circ 20') = \pm 158^\circ 40' \end{aligned}$$

Case 2

$$\begin{aligned} \omega t &= 2 \sin^{-1} \left[ \frac{1 + \tan 39^\circ \tan 29^\circ}{2} \right]^{1/2} \\ &= 2 \sin^{-1} \left[ \frac{1 + 0.80978 \cdot 0.55431}{2} = 0.72443 \right]^{1/2} \\ &= 2 \sin^{-1} 0.85114 = 2(\pm 58^\circ 20') = \pm 116^\circ 40' \end{aligned}$$

The maximum elevation angle was originally chosen as  $80^\circ$  for both cases.

## ELEVATION ANGULAR VELOCITY AND ACCELERATION

Take the derivative of Eq. (12) to obtain the elevation angular velocity as follows:

$$\cos h \frac{dh}{dt} = -D \omega \sin \frac{\omega t}{2} \cos \frac{\omega t}{2} \quad (16)$$

$$\frac{dh}{dt} = \pm \frac{D \omega \sin \omega t}{2\sqrt{1 - (C - D \sin^2 \frac{\omega t}{2})^2}} \quad (17)$$

$$= \pm \frac{D \omega \sin \omega t}{[4 - (2C - D + D \cos \omega t)^2]^{1/2}} \quad (18)$$

For purposes of numerical evaluation of  $h$ ,  $\dot{h}$ , and  $\ddot{h}$  as a function of time, the alternative form may be used for elevation angular rate as given by

$$\frac{dh}{dt} = - \frac{D \omega \sin \omega t}{2 \cosh h} \quad (19)$$

Figure 4 shows elevation angle and angular rate as a function of time for both Case 1 and Case 2.

Elevation angular acceleration is found by taking the derivative of Eq. (19). Thus,

$$\frac{d^2h}{dt^2} = \ddot{h} = - \frac{D\omega}{2\cos^2 h} (\omega \cos h \cos \omega t + \sin \omega t \sinh h \frac{dh}{dt}) \quad (20)$$

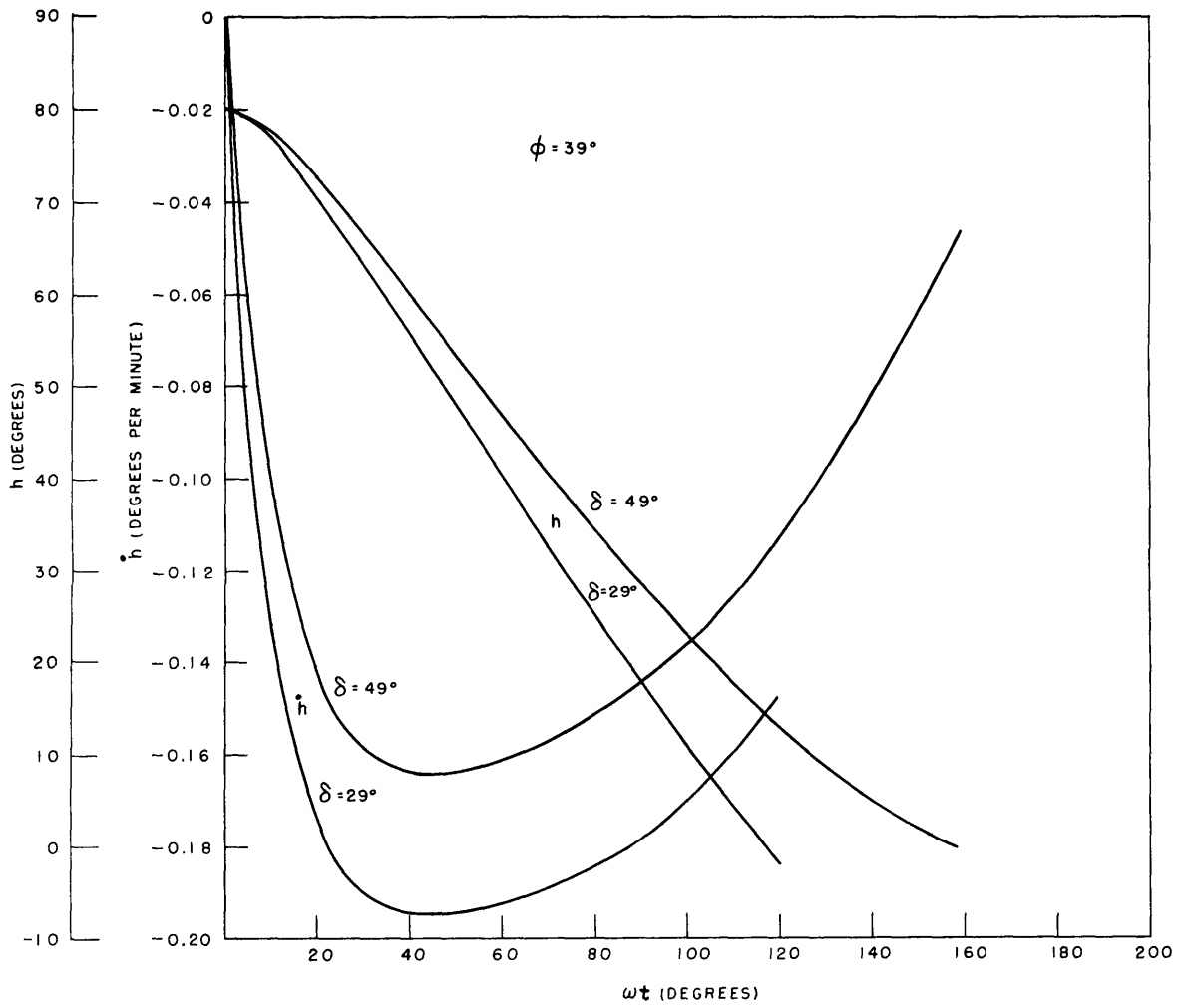


Fig. 4 -  $h$  and  $\dot{h}$  versus  $\omega t$  for Case 1 and Case 2

The points of maximum and minimum velocity are found by setting acceleration equal to zero. Accordingly,

$$\omega \cos h \cos \omega t + \sin \omega t \sin h \frac{dh}{dt} = 0 \quad (21)$$

$$\omega \cos h \cos \omega t = \frac{D \omega \sin^2 \omega t \sin h}{2 \cos h} \quad (22)$$

$$\frac{\cos \omega t}{\sin^2 \omega t} = \frac{D \sin h}{2 \cos^2 h} \quad (23)$$

$$\sin h - \frac{l}{\sin h} = \cos \phi \cos \delta \left( \cos \omega t - \frac{l}{\cos \omega t} \right) \quad (24)$$

Trial of values in the neighborhood of  $\omega t = 45^\circ$  were made using Eq. (24) as the measure, with the result for Case 2 that

$$\omega t \Big|_{\max h} \approx \pm 47.15 \text{ degrees} \quad (25)$$

and, substituting into Eq. (12), Eq. (19), and Eq. (20),

$$h \Big|_{\max h} \approx \pm 50.23 \text{ degrees} \quad (26)$$

$$\dot{h} \Big|_{\max h} \approx \mp 0.1943 \text{ degrees per minute} \quad (27)$$

$$\ddot{h} \Big|_{\max h} = 0$$

The minimum value for angular velocity in the elevation coordinate is zero at transit ( $\omega t = 0$ ,  $h = 80^\circ$ ).

A region of near-zero elevation rate occurs near maximum elevation.

Maximum acceleration (positive rate of change of velocity) in the elevation coordinate occurs at the horizon ( $h = 0$ ) where  $\omega t = \pm 158^\circ 40'$  for Case 1 and  $\omega t = \pm 116^\circ 40'$  for Case 2. Using Eq. (20), we obtain

$$\left. \frac{d^2 h}{dt^2} \right|_{\text{max accel}} = \ddot{h} \Big|_{\text{max accel}} = -\omega^2 \cos \phi \cos \delta \cos \omega t \quad (28)$$

Case 1

$$\phi = 39^\circ$$

$$\delta = 49^\circ$$

$$\ddot{h} \Big|_{\text{max accel}} = -1/16 \cos 39^\circ \cos 49^\circ \cos 158^\circ 40'$$

$$= 0.77715 \cdot 0.65606 \cdot 0.93144$$

$$= 0.0297 \text{ degree per minute per minute}$$

Case 2

$$\phi = 39^\circ$$

$$\delta = 29^\circ$$

$$\ddot{h} \Big|_{\text{max accel}} = -1/16 \cos 39^\circ \cos 29^\circ \cos 116^\circ 40'$$

$$= \frac{0.77715 \cdot 0.87462 \cdot 0.44870}{16}$$

$$= 0.01906 \text{ degree per minute per minute}$$

## FREQUENCY DOMAIN EQUIVALENT OF AZIMUTH TIME FUNCTION

Figure 3 may be interpreted as a time-domain specification of the problem of azimuth tracking imposed by the motion of the hypothetical star represented by Case 2. For the purposes of servo system design, the frequency domain transformation of this time function is desired. This transformation is obtained by Guillemin's impulse method (1,5), in which the integrand of the Laplace integral is converted to a set of impulses in order that the integral may be evaluated without numerical methods. Steps in the application of the method are indicated on Fig. 5. The position of the time function that lies between star rise and star set is replotted in Fig. 5a, taking the new origin of coordinates at the time and azimuth angle of star rise.

To obtain the set of impulses, the derivative of the time function is first plotted, Fig. 5b, and approximated by a broken line (this approximation is equivalent to fitting the time function with a series of parabolic segments). The broken line approximation is then differentiated twice, Fig. 5c and 5d, to obtain a set of impulses. The change in units from radians/second<sup>2</sup> to radians/second<sup>3</sup> associated with the taking of the third derivative is offset by the fact that the indicated strengths are related to areas with time as the abscissa. The impulses shown in Fig. 5d are an approximation representing the information within the interval between star rise and star set with the assumption that a continuous function is involved. That is,  $\theta$ ,  $\dot{\theta}$ ,  $\ddot{\theta}$ , etc., have the same value immediately prior to the star rise point ( $t=0$ ) as immediately after. In like manner, the function is also continuous at the end, i.e., at star set.

Appendix A contains the details of the mathematical processing from the impulses of Fig. 5d to the continuous frequency domain equivalent shown in Fig. 6.

## AZIMUTH SERVO SYSTEM TRANSFER FUNCTION

In the Graham design procedure (2), use is made of a steady-state error series having the general form

$$\epsilon_{ss} = \frac{\theta_i}{1 + K_p} + \frac{\dot{\theta}_i}{K_v} + \frac{\ddot{\theta}_i}{K_a} + \frac{\ddot{\theta}_i}{K_a} + \dots$$

where

$$K_p = \text{position error constant}$$

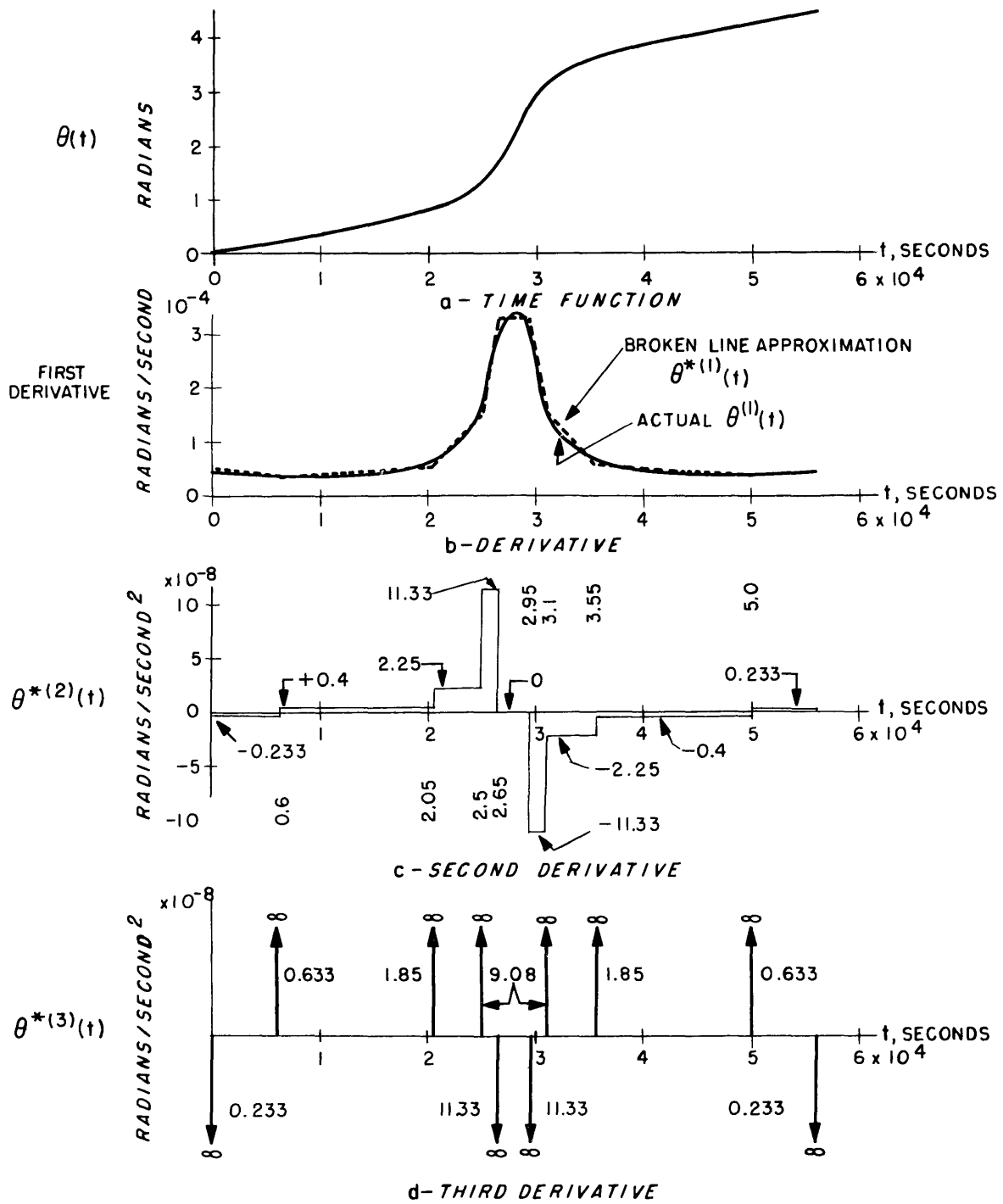


Fig. 5 - Derivatives of the time function in the approximation process

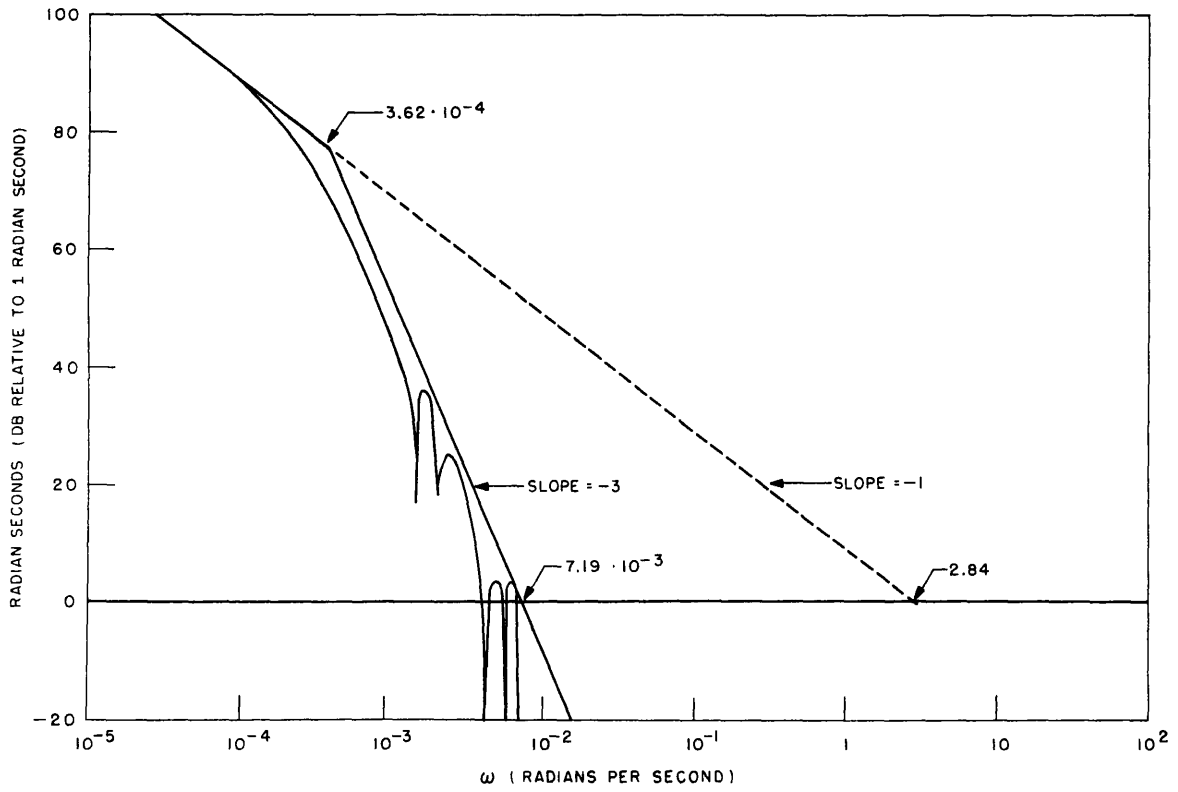


Fig. 6 - Azimuth excitation function transformed into the frequency domain

$K_v$  = velocity error constant

$K_a$  = acceleration error constant

$K_{\ddot{a}}$  = rate of change of acceleration error constant

Anticipating need for information regarding the input motion and its derivatives, expressions for  $\theta_i$ ,  $\dot{\theta}_i$ , and  $\ddot{\theta}_i$  were derived and appear earlier in the report. Variations in design predicated upon higher derivatives than the second (acceleration) should be avoided (6).

Study of Fig. 6 leads to the choice of the servo system transfer characteristic shown in Fig. 7. The low-frequency asymptotic slope of -1 is followed by a high-frequency asymptotic slope of -2 with unity gain at the break frequency (7). For such a system, the steady-state error expression is

$$\epsilon_{ss} \cong \frac{\dot{\theta}_i}{\omega_1} \quad (30)$$

The maximum required bandwidth, i.e., maximum value for  $\omega_1$ , is found by using the maximum value of input velocity in Eq. (30). For an assumed specification of  $1/4^\circ$  maximum allowable error,  $\omega_1 = 0.084$ . Thus, a bandwidth of 0.1 radian per second is adequate for the train axis. If the tracking accuracy requirements had been lower, less of an "overcoat fit" of the excitation function shown in Fig. 6 would have resulted.

#### AUTOMATIC TRACKING REQUIREMENTS STARTING FROM REST

Consider a radio star tracking system in which the antenna feed point is nutated to permit development of an error signal. For such a system it would be possible to demand of the servo system an ability to start from initial conditions in which an error in  $\theta$ ,  $\dot{\theta}$ ,  $\ddot{\theta}$ , etc., exists.

The function shown in Fig. 6 is based upon zero initial errors. To illustrate the effect of an error, consider the initial conditions (where the minus and plus subscripts refer to the instant before and the instant after the transient)

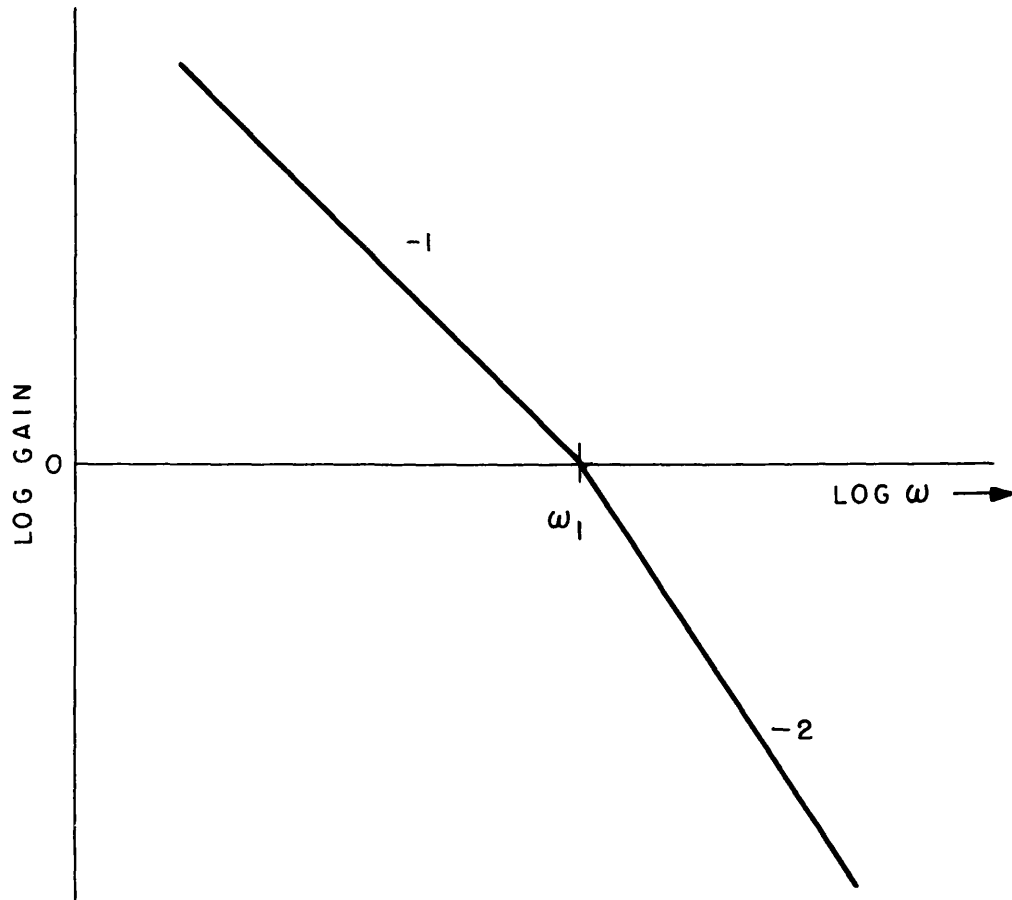


Fig. 7 - Type I servo system open-loop asymptotic characteristics

$\theta_- = \theta_+$  , as in Fig. 5a

$\dot{\theta}_-$  ,  $\ddot{\theta}_-$  , etc. = 0

$\dot{\theta}_+$  ,  $\ddot{\theta}_+$  , etc., same as in Fig. 5a

The effect of initial conditions is to introduce an impulse at  $t = 0$  in Fig. 5c which becomes a doublet (8) in Fig. 5d. The strength is established by the step at  $t = 0$  in Fig. 5b, i.e., +0.473. The approximation of the transform of the time function is

$$\begin{aligned} \Theta^*(j\omega) &= \text{Rt. side Eq. (A1)} + \frac{0.473 \cdot 10^{-4}}{(j\omega)^2} = \text{Rt. side Eq. (A7)} - \frac{0.473 \cdot 10^4}{F^2} \\ &= -10^4 \left\{ \left[ \frac{0.473}{F^2} + \frac{G \sin 2.8F}{F^3} \right] + j \left[ \frac{G \cos 2.8F}{F^3} \right] \right\} \end{aligned} \quad (31)$$

The magnitude of Eq. (31) is given by

$$|\Theta^*(j\omega)| = 10^4 \left\{ \frac{0.473^2}{F^4} + \frac{2 \cdot 0.473 G \sin 2.8F}{F^5} + \frac{G^2}{F^6} \right\}^{1/2} \quad (32)$$

The zero frequency asymptotic function is

$$|\Theta^*(j\omega)|_{F \rightarrow 0} = \frac{0.473 \cdot 10^4}{F^2} = \frac{68.78^2}{F^2} = \left[ \frac{6.878 \cdot 10^{-3}}{\omega} \right]^2 \quad (33)$$

as compared with the  $2.84 \cdot 10^4$ ; F function given in Eq. (A11) where no starting transient servo requirements are involved. If such a servo system is desired, the excitation function represented by Eq. (32) may be studied in the same manner as Eq. (A8). The transfer characteristic should be a Type II, that is, one in which the initial asymptotic slope is -2, followed by a mid-frequency asymptotic slope of -1, and ending with a high-frequency -2 slope (9).

#### PROPOSED SERVO SYSTEM

Figure 8 shows, in block diagram form, a possible servo system arrangement for the automatic star tracking problem in azimuth in which elimination of errors due to initial transients is not required -- the

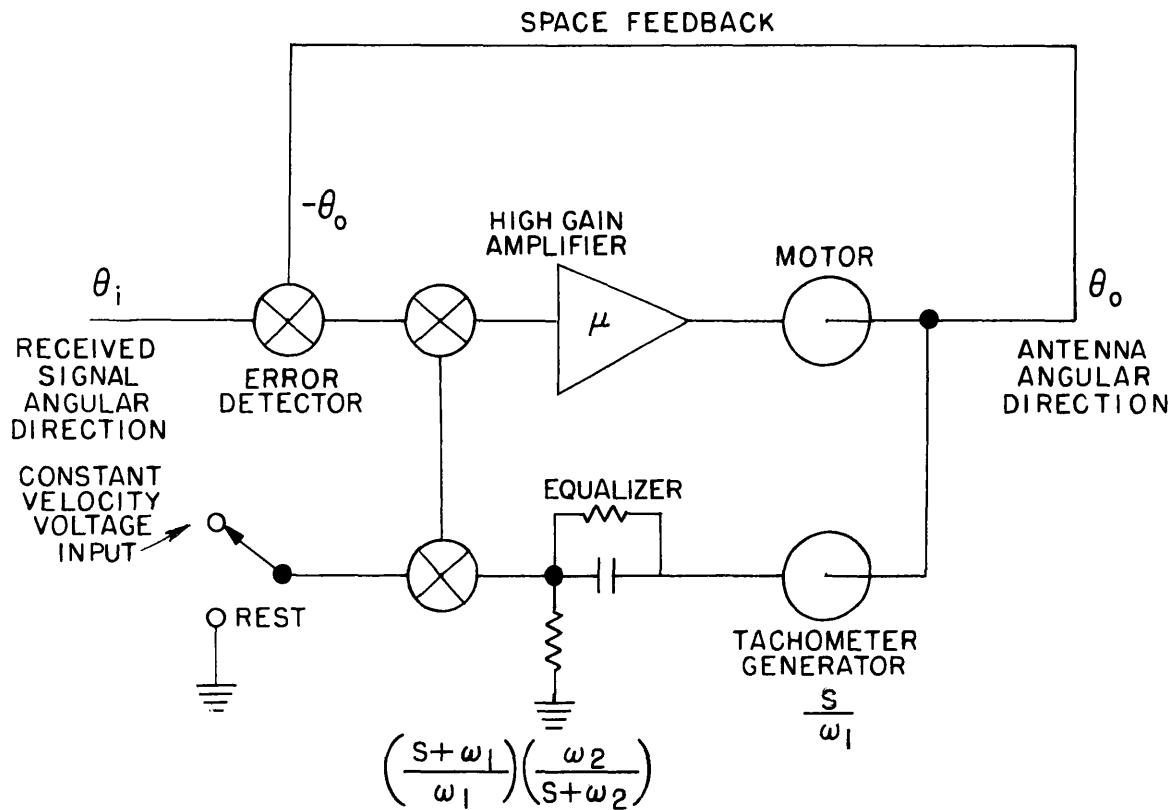


Fig. 8 - Block diagram for azimuth servo system

problem and system of Figs. 5, 6, and 7. The error expression for the system shown is substantially identical to Eq. (30).

The switch shown in Fig. 8 provides a means whereby the antenna may be held in a fixed position until tracking is desired. The introduction of a fixed voltage corresponding to a selectable constant angular velocity reduces the servo tracking problem to tracking the difference instead of the total. The  $\omega_2$  of the equalizer should be approximately  $10 \omega_1$  or 1 radian per second.

### CONCLUSIONS

Star tracking with an elevation-azimuth coordinate system has been studied. Time functions have been given for position, velocity, and acceleration components in both axes. Details of the transformation to the frequency domain equivalent and the design of a suitable servo system for the azimuth axis are included. A bandwidth of 0.1 radian per second is shown to be adequate for the azimuth servo system. A proposed system is shown in block diagram form.

#### REFERENCES

1. Guillemin, E. A., "Computational Techniques which Simplify the Correlation between Steady-State and Transient Responses of Filters and Other Networks," Proc. Nat. Electronics Conf. 1953, 9:513-532, 1954
2. Graham, R. E., "Linear Servo Theory," Bell System Tech. J., 25: 616-651, October 1946
3. Truxal, J. G., "Automatic Feedback Control System Synthesis," New York:McGraw-Hill, pp. 80-87, 1955
4. Hosmer, G. L., "Practical Astronomy," New York:John Wiley, 3rd Edition, 1925
5. Truxal, pp. 379-382
6. Truxal, p. 284
7. Locke, A.S., "Guidance," New York:D. Van Nostrand, pp. 236-245, 1955
8. Truxal, p. 55
9. Locke, pp. 255-259

APPENDIX A

TIME DOMAIN TO FREQUENCY DOMAIN TRANSFORMATION

The approximation of the transform of the time function shown in Fig. 5 is

$$\begin{aligned} \Theta^*(j\omega) = \frac{10^{-8}}{(j\omega)^3} & \left[ -0.233 + 0.633 e^{-j\omega 0.6 \cdot 10^4} \right. \\ & + 1.85 e^{-j\omega 2.05 \cdot 10^4} + 9.08 e^{-j\omega 2.5 \cdot 10^4} - 11.33 e^{-j\omega 2.65 \cdot 10^4} \\ & - 11.33 e^{-j\omega 2.95 \cdot 10^4} + 9.08 e^{-j\omega 3.1 \cdot 10^4} + 1.85 e^{-j\omega 3.55 \cdot 10^4} \\ & \left. + 0.633 e^{-j\omega 5 \cdot 10^4} - 0.233 e^{-j\omega 5.6 \cdot 10^4} \right] \end{aligned} \quad (A1)$$

Writing the exponentials in the form of in-phase and quadrature components, we have

$$\begin{aligned} \Theta^*(j\omega) = \frac{10^{-8}}{-j\omega^3} & \left[ -0.233 + 0.633 (\cos 0.6 \cdot 10^4 \omega - j \sin 0.6 \cdot 10^4 \omega) \right. \\ & + 1.85 (\cos 2.05 \cdot 10^4 \omega - j \sin 2.05 \cdot 10^4 \omega) + 9.08 (\cos 2.5 \cdot 10^4 \omega - j \sin 2.5 \cdot 10^4 \omega) \\ & - 11.33 (\cos 2.65 \cdot 10^4 \omega - j \sin 2.65 \cdot 10^4 \omega) - 11.33 (\cos 2.95 \cdot 10^4 \omega - j \sin 2.95 \cdot 10^4 \omega) \\ & + 9.08 (\cos 3.1 \cdot 10^4 \omega - j \sin 3.1 \cdot 10^4 \omega) + 1.85 (\cos 3.55 \cdot 10^4 \omega - j \sin 3.55 \cdot 10^4 \omega) \\ & \left. + 0.633 (\cos 5 \cdot 10^4 \omega - j \sin 5 \cdot 10^4 \omega) - 0.233 (\cos 5.6 \cdot 10^4 \omega - j \sin 5.6 \cdot 10^4 \omega) \right] \end{aligned} \quad (A2)$$

Introducing a reference angular frequency  $\omega_0 = 10^{-4}$  radian per second and letting  $F = \omega/\omega_0$ , we have

$$\begin{aligned} \Theta^*(j\omega) = & -\frac{10^4}{F^3} \left\{ \left[ -0.233 \sin 0.6F + 0.633 \sin 0.6F \right. \right. \\ & + 1.85 \sin 2.05F + 9.08 \sin 2.5F - 11.33 \sin 2.65F - 11.33 \sin 2.95F \\ & + 9.08 \sin 3.1F + 1.85 \sin 3.55F + 0.633 \sin 5F - 0.233 \sin 5.6F \left. \right] \\ & + j \left[ -0.233 \cos 0.6F + 0.633 \cos 0.6F + 1.85 \cos 2.05F \right. \\ & + 9.08 \cos 2.5F - 11.33 \cos 2.65F - 11.33 \cos 2.95F \\ & + 9.08 \cos 3.1F + 1.85 \cos 3.55F + 0.633 \cos 5F \\ & \left. \left. - 0.233 \cos 5.6F \right] \right\} \quad (A3) \end{aligned}$$

$$\begin{aligned} = & -\frac{10^4}{F^3} \left\{ \left[ -0.233 (\sin 0.6F + \sin 5.6F) \right. \right. \\ & + 0.633 (\sin 0.6F + \sin 5F) + 1.85 (\sin 2.05F + \sin 3.55F) \\ & + 9.08 (\sin 2.5F + \sin 3.1F) - 11.33 (\sin 2.65F + \sin 2.95F) \left. \right] \\ & + j \left[ -0.233 (\cos 0.6F + \cos 5.6F) \right. \\ & + 0.633 (\cos 0.6F + \cos 5F) + 1.85 (\cos 2.05F + \cos 3.55F) \\ & + 9.08 (\cos 2.5F + \cos 3.1F) - 11.33 (\cos 2.65F + \cos 2.95F) \left. \right] \left. \right\} \quad (A4) \end{aligned}$$

$$\Theta^*(j\omega) = -\frac{10^{-4}}{F^3} \left\{ \sin 2.8F + j \cos 2.8F \right\} (-G) \quad (A5)$$

where

$$\begin{aligned} G = & 0.466 \cos 2.8F - 1.266 \cos 2.2F \\ & - 3.7 \cos 0.75F - 18.16 \cos 0.3F \\ & + 22.66 \cos 0.15F \quad (A6) \end{aligned}$$

$$\theta^*(j\omega) = \frac{10^4 G}{F^3} (\sin 2.8 F + j \cos 2.8 F) \quad (A7)$$

The magnitude becomes

$$|\theta^*(j\omega)| = \left| \frac{10^4 G}{F^3} \right| \quad (A8)$$

Before numerical evaluation is made of Eq. (A7) as a function of frequency, consider its nature as frequency approaches zero. The expansion

$$\cos x = 1 - \frac{x^2}{2!} + \dots \quad (A9)$$

may be used in evaluating G for  $F \rightarrow 0$ . Thus,

$$\begin{aligned} \lim_{F \rightarrow 0} |G| &= \lim_{F \rightarrow 0} \left| +0.466 \left(1 - \frac{2.8 F^2}{2}\right) \right. \\ &\quad \left. -1.266 \left(1 - \frac{2.2 F^2}{2}\right) - 3.7 \left(1 - \frac{0.75 F^2}{2}\right) \right. \\ &\quad \left. -18.16 \left(1 - \frac{0.3 F^2}{2}\right) + 22.66 \left(1 - \frac{0.15 F^2}{2}\right) \right| \\ &= \frac{F^2}{2} (0.466 \cdot 2.8^2 - 1.266 \cdot 2.2^2 \\ &\quad - 3.7 \cdot 0.75^2 - 18.16 \cdot 0.3^2 + 22.66 \cdot 0.15^2) \quad (A10) \end{aligned}$$

Substitution of Eq. (A10) into Eq. (A7) yields

$$\begin{aligned} \lim_{F \rightarrow 0} |\theta^*(j\omega)| &= \left| \frac{0.466 \cdot 2.8^2 - 1.266 \cdot 2.2^2 - 3.7 \cdot 0.75^2 - 18.16 \cdot 0.3^2 + 22.66 \cdot 0.15^2}{2 \cdot 10^{-4} F} \right| \\ &= \frac{2.84 \cdot 10^4}{F} = \frac{2.84}{\omega} \end{aligned}$$

Equation (A11) shows that the excitation function frequency domain equivalent, when plotted on log-log scales, has a minus one slope as the frequency approaches zero. This minus one slope extended has a value of unity at a frequency  $F = \frac{\omega}{\omega_0} = \frac{\omega}{10^{-4}} = 2.84 \cdot 10^4$  or  $\omega = 2.84$ .

The series expansion of the cosine functions fails to facilitate similar determination of the high-frequency asymptote. Instead, the cyclic nature of Eq. (A7) must be considered and a determination of the peak value made. The asymptotes are tangent near the peak values. The function itself makes cyclic excursion to zero or minus infinity on the log plot. Hence, the asymptotes must be regarded as defining the upper limit of the function.

Repeating Eq. (A6),

$$-G = \left[ -0.466 \cos 2.8 F + 1.266 \cos 2.2 F + 3.7 \cos 0.75 F + 18.16 \cos 0.3 F - 22.66 \cos 0.15 F \right] \quad (A12)$$

may be rewritten as

$$-G = -0.466 \cos\left(\frac{F}{\tau_1}\right)2\pi + 1.266 \cos\left(\frac{F}{\tau_2}\right)2\pi + 3.7 \cos\left(\frac{F}{\tau_3}\right)2\pi + 18.16 \cos\left(\frac{F}{\tau_4}\right)2\pi - 22.66 \cos\left(\frac{F}{\tau_5}\right)2\pi \quad (A13)$$

where

$$\tau_1 = \frac{2\pi}{2.8}, \quad \tau_2 = \frac{2\pi}{2.2}, \quad \tau_3 = \frac{2\pi}{0.75}, \quad \tau_4 = \frac{2\pi}{0.30}, \quad \text{and} \quad \tau_5 = \frac{2\pi}{0.15}$$

Considering the factor  $2\pi$  separately, express the fractions using the least common denominator as follows:

$$\frac{1}{2.8}, \quad \frac{1}{2.2}, \quad \frac{1}{0.75}, \quad \frac{1}{0.30}, \quad \frac{1}{0.15} \quad (A14)$$

become

$$\frac{165}{462}, \quad \frac{210}{462}, \quad \frac{616}{462}, \quad \frac{1540}{462}, \quad \frac{3080}{462} \quad (A15)$$

The number of cycles of each frequency in the composite period is found by determination of the least common multiple of the numerators of the ratios (A15). Thus, the numbers

$$165, 210, 616, 1540, 3080 \quad (A16)$$

lead to

$$56 \cdot 165, 44 \cdot 210, 15 \cdot 616, 6 \cdot 1540, 3 \cdot 3080 \quad (A17)$$

The products (A17) show that the number of cycles of each cosine term of Eq. (A7) in the period of the combination is 56, 44, 15, 6, and 3 respectively. The relative importance of the terms progresses downward as frequency increases. Since the sign of the two low-frequency terms are opposite, the value of F for which they are out of phase appears to be a region where a maximum occurs.

In the general case great difficulty may be experienced in locating the region of the peak value. Setting the derivative of G equal to zero results in a sum of sine terms with the desired value of F implicit. A series expansion of the cosine terms in G prior to taking the derivative changes the problem to a solution of a high order polynomial which, since it is based upon a limited number of terms of the series, gives only approximate answers.

A simple, easily applied, procedure consists of setting up as many rows as terms (five in the present example) and providing columns in which the location of the maximum positive and the maximum negative value may be indicated for all cycles of each cosine term. The point of favorable coincidence can be established through scanning by eye. This was done for the example using the following:

Columns per cycle	Term
220	cos 0.15 F
110	cos 0.30 F
44	cos 0.75 F
15	cos 2.2 F
$165/14 \cong 11.78$	cos 2.8 F

As it developed, the composite function showed symmetry about the half-cycle point and the process was completed using 330 columns. The non-integral columns per cycle for the highest frequency term caused no particular difficulty. At columns 110 and 550 a value 36.487 was found. The peak occurs at column 330 with the value 37.92.

Equation (A8) may be regarded as having two parts. The denominator gives rise to a -3 slope on a log-log plot. The remaining problem is to locate this -3 slope so that tangency with the cyclic numerator is obtained. The numerator will have a -3 slope (on a log-log plot) at the points of tangency. Proceed by setting

$$\frac{d(10^4 G)}{d \log_{10} F} = -3 \quad (A18)$$

$$\begin{aligned} &= \frac{\frac{1}{10^4 G} \log_{10} \epsilon \cdot \frac{d}{dF}(10^4 G) dF}{\frac{1}{F} \log_{10} \epsilon \cdot dF} = -3 \\ &= \frac{F \frac{d}{dF}(10^4 G)}{(10^4 G)} = -3 \end{aligned} \quad (A19)$$

Substitution of Eq. (A6) for G leads to

$$\begin{aligned} -3 &= F \cdot 10^4 \left[ -0.466 \cdot 2.8 \sin 2.8 F + 1.266 \cdot 2.2 \sin 2.2 F \right. \\ &\quad \left. + 3.7 \cdot 0.75 \sin 0.75 F + 18.16 \cdot 0.3 \sin 0.3 F \right. \\ &\quad \left. - 22.66 \cdot 0.15 \sin 0.15 F \right] \\ &\div 10^4 \left[ 0.466 \cos 2.8 F - 1.266 \cos 2.2 F \right. \\ &\quad \left. - 3.7 \cos 0.75 F - 18.16 \cos 0.3 F \right. \\ &\quad \left. + 22.66 \cos 0.15 F \right] \end{aligned} \quad (A20)$$

$$\begin{aligned} \frac{3}{F} &= (1.3048 \sin 2.8 F - 2.7852 \sin 2.2 F - 2.775 \sin 0.75 F \\ &\quad - 5.448 \sin 0.3 F + 3.399 \sin 0.15 F) \div (0.466 \cos 2.8 F \\ &\quad - 1.266 \cos 2.2 F - 3.7 \cos 0.75 F - 18.16 \cos 0.3 F + 22.66 \cos 0.15 F) \end{aligned} \quad (A21)$$

The equality of interest is, as already established, in the region

$$F = 1.5 \frac{2\pi}{0.15} = 20\pi = 62.83185 \quad (\text{A22})$$

Trial and error yields the approximation

$$F = 63.5748 \quad (\text{A23})$$

For  $F = 63.5748$ , Eq. (A8) gives

$$\left| \theta^*(j\omega) \right|_{F=63.5748} = 1.449 = +3.22 \text{ db} \quad (\text{A24})$$

The next point of tangency occurs one cycle later or for

$$F = 63.5748 + 125.6637 = 189.2385 \quad (\text{A25})$$

at which

$$\left| \theta^*(j\omega) \right|_{F=189.2385} = 5.495 \cdot 10^{-2} = -25.20 \text{ db} \quad (\text{A26})$$

The high-frequency asymptote crosses unity gain at

$$\begin{aligned} F^3 &= 37.23745 \cdot 10^4 = .3723745 \cdot 10^6 \\ F &= 71.94 \\ \omega &= 7.194 \cdot 10^{-3} \end{aligned} \quad (\text{A27})$$

Therefore, the equation of the high-frequency asymptote is

$$\lim_{F \rightarrow \infty} \left| \theta^*(j\omega) \right| = \frac{37.237 \cdot 10^4}{F^3} = \frac{37.237 \cdot 10^{-8}}{\omega^3} \quad (\text{A28})$$

The low-frequency asymptote intersects the high-frequency asymptote at

$$F = \left[ \frac{(7.194 \cdot 10^{-3})^3}{2.84} \right]^{1/2} = 3.62 \cdot 10^{-4} \quad (\text{A29})$$

The function, as given by Eq. (A8), and the asymptotes, as given by Eq. (A11) and Eq. (A28), are plotted in Fig. 6.

The high-frequency asymptotic slope of -3 results from the three derivatives in the approximation process. If, instead of one derivative before the broken-line approximation, two derivatives had been taken, then the high-frequency asymptotic slope would have been -4. Clearly, since the final high-frequency slope is a function of the total number of derivatives taken, the actual slope has no significance. In looking at the entire curve of Fig. 6 then, one must keep in mind that the relative accuracy is highest at the low-frequency end and drops to zero as the final slope is reached. Since servo systems with greater than -2 slope (through unity gain) become unstable, sufficient accuracy for the present purposes is provided in Fig. 6.